Liquid Crystals
Publication details, including instructions for authors and subscription information:
http://www.informaworld.com/smpp/title~content=t713926090

Non-symmetric liquid crystal dimers containing the 4-nitrobenzohydrazide group: synthesis and mesomorphic behaviour

Binglian Bai[a][b]; Haitao Wang[a]; Peng Zhang[a]; Songnan Qu[a]; Fan Li[a]; Zhixin Yu[a]; Beihong Long[a]; Min Li[a]
[a] Key Laboratory for Automobile Materials (JLU), Ministry of Education, Institute of Materials Science and Engineering, Jilin University, Changchun 130012, P.R. China [b] College of Physics, Jilin University, Changchun 130023, P.R. China

To cite this Article Bai, Binglian , Wang, Haitao , Zhang, Peng , Qu, Songnan , Li, Fan , Yu, Zhixin , Long, Beihong and Li, Min(2008) 'Non-symmetric liquid crystal dimers containing the 4-nitrobenzohydrazide group: synthesis and mesomorphic behaviour', Liquid Crystals, 35: 7, 793 — 798

To link to this Article: DOI: 10.1080/02678290802187264

URL: http://dx.doi.org/10.1080/02678290802187264

Liquid Crystals,
Vol. 35, No. 7, July 2008, 793–798

Taylor & Francis
Taylor & Francis Group

Non-symmetric liquid crystal dimers containing the 4-nitrobenzohydrazide group: synthesis and mesomorphic behaviour

Binglian Bai[ab], Haitao Wang[a], Peng Zhang[a], Songnan Qu[a], Fan Li[a], Zhixin Yu[a], Beihong Long[a] and Min Li[a]*

[a] *Key Laboratory for Automobile Materials (JLU), Ministry of Education, Institute of Materials Science and Engineering, Jilin University, Changchun 130012, P.R. China;* [b] *College of Physics, Jilin University, Changchun 130023, P.R. China*

(Received 29 December 2007; final form 7 May 2008)

The synthesis and mesomorphic behaviour are reported of a new series of dimers containing 4-nitrobenzohydrazide and azobenzene groups as the mesogenic units. These non-symmetric liquid crystal dimers are found to exhibit a monolayer smectic A phase (SmA_1). Lateral hydrogen bonding and strong dipole–dipole interactions are shown to be the major driving forces for the formation of the SmA_1 phase. The present study indicates that the intermolecular interactions and thus the mesophase morphology of the liquid crystal dimers can be controlled by the appropriate selection of the molecular fragments capable of forming H-bonds.

Keywords: liquid crystal dimers; hydrogen bonding; hydrazide; derivatives; azobenzene

1. Introduction

Liquid crystal dimers, which contain either two identical (symmetric) or non-identical (non-symmetric) mesogenic units connected via a flexible central spacer (*1–3*), have attracted increasing attention not only because they are regarded as model compounds for polymeric liquid crystals, but also due to their inherently interesting liquid crystalline properties (*4–7*). There are remarkable differences in the mesophase behaviour of non-symmetric and symmetric dimers. Non-symmetric liquid crystal dimers usually exhibit intercalated smectic phases, in which specific molecular interactions between the two different mesogenic units account for this specific phase behaviour (*8–10*). In contrast, the symmetric liquid crystal dimers exhibiting smectic phases have a strong tendency to exhibit monolayer smectic phases (*2*). In general, the mesophase behaviour of liquid crystal dimers depends on several factors, such as the structure and size of the mesogenic units and the chemical structure and the length of the spacers and terminal groups (*11–14*).

It has been demonstrated that intermolecular hydrogen bonding plays an important role in mesophase formation in hydrazide derivatives (*15–18*). We have confirmed that lateral intermolecular hydrogen bonding occurred in the smectic A (SmA) phase and played an important role in stabilising the mesophase of non-symmetric hydrazide derivatives (**Cn-NO$_2$**) (*19*). Furthermore, we have reported symmetric liquid crystal dimers (**N$_n$**) (*20*) and non-symmetric liquid crystal dimers (**EmCn**, scheme 1) (*21*) containing hydrazide groups, where lateral intermolecular hydrogen bonding was demonstrated to be the driving force for the intercalated smectic phase as well as the monolayer smectic C phases.

In this paper, the synthesis, phase behaviour and mesophase structures are reported for non-symmetric liquid crystal dimers containing the 4-nitrobenzohydrazide group, i.e. 1-[4-(4′-alkoxyphenylazo)phenoxy]-*n*-[(*N*-(4-nitrobenzoyl)-*N*′-(benzoyl-4′-oxy)hydrazine)]alkane (**Ep-m-NO$_2$**) (see Scheme 1), in which the hydrazide group was expected to increase the intermolecular interaction between the mesogenic units; the nitro (–NO$_2$) group was used to introduce strong longitudinal dipole-dipole interactions. In addition, the dependence of the phase behaviours on length of the spacer and the terminal alkoxy chains was investigated. The results of these studies contribute to an understanding the structure–property relationships of liquid crystal dimers.

2. Experimental

Synthesis

The target non-symmetric dimers, **Ep-m-NO$_2$** (where **m** signifies the number of methylene units in the spacer and **p** indicates the number of methylene units in the terminal alkoxy tail of the azobenzene core), were synthesised through the route shown in Scheme 2. 4-{*m*-[4-(4-Alkoxyphenylazo)phenoxy]alkoxy}benzoic acid was prepared according to a method described previously (*22*) and the target products were obtained through the reaction of 4-{*m*-[4-(4-methoxyphenylazo)-phenoxy]alkoxy}-benzoic chloride (**Ep-m**) and 4-nitrobenzoylhydrazine in pyridine at 40°C. All the

---

*Corresponding author. Email: minli@jlu.edu.cn

ISSN 0267-8292 print/ISSN 1366-5855 online

DOI: 10.1080/02678290802187264
http://www.informaworld.com

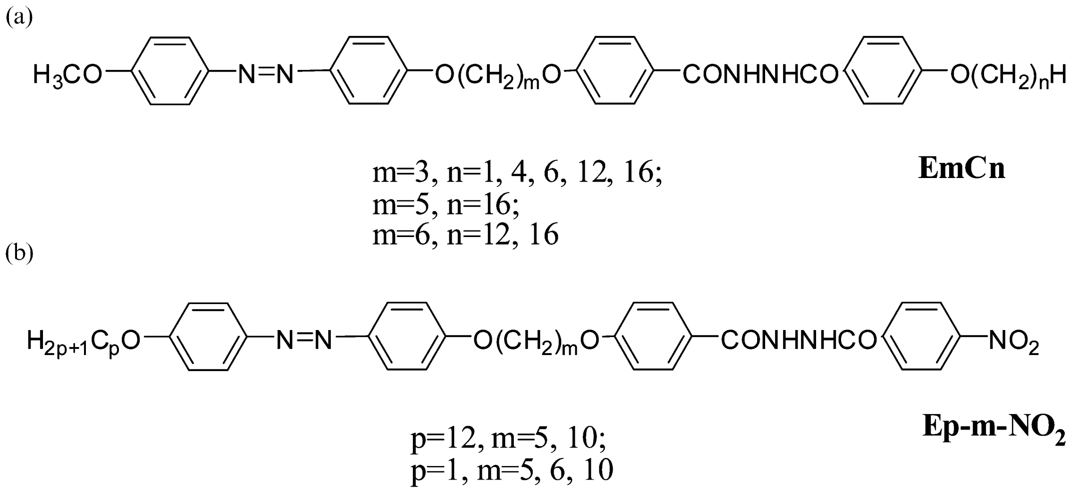

Scheme 1. The molecular structures of non-symmetric liquid crystal dimers (a) **EmCn** (*21*) and (b) **Ep-m-NO$_2$**.

compounds were purified by recrystallisation from DMF for further ^{1}H NMR measurements, FTIR and elemental analysis. (Because of its poor solubility, a ^{1}H NMR experiment was not performed for **Ep-10-NO$_2$**).

*1-[4-(4′-Dodecyloxyphenylazo)phenoxy]-5-[(N-(4-nitrobenzoyl)-N′-(benzoyl-4-oxy)hydrazine)]pentane (**E12-5-NO$_2$**).*

4-{5-[4-(4-Dodecyloxyphenylazo)phenoxy]pentyloxy} benzoic acid (1.32 g, 0.0022 mol) and thionyl chloride (50 ml) were refluxed for 5 h. 4-{5-[4-(4-Dodecyloxyphenylazo)phenoxy]pentyloxy}benzoic chloride (**E12-5**) was collected after removing the unreacted thionyl chloride. Then, 4-{5-[4-(4-dodecyloxyphenylazo)phenoxy]pentyloxy}benzoic chloride was dissolved in pyridine (100 ml) and was stirred at 40°C; 4-nitrobenzoylhydrazine (0.41 g, 0.0022 mol) was added slowly, and the resulting mixture was stirred for 8 h. The reaction mixture was poured into an excess of ice water, and the precipitate recrystallised from DMF. ^{1}H NMR (300 MHz, DMSO): δ 0.83–0.87 (t, 3H, –C–CH$_3$), 1.24–1.61 (m, 20H, –C–(CH$_2$)$_9$–C and –O–C–C–CH$_2$–C–C–O–), 1.74 (m, 2H, –O–C–CH$_2$–C–C), 1.84 (m, 4H, –O–C–CH$_2$–C–CH$_2$–C–O–), 4.04–4.11 (t, 6H, –O–CH$_2$–C–CH$_2$–O– and –O–CH$_2$–C–C–), 7.06–7.08(m, 2H, Ar–H, *m*-to, –CON–), 7.10–7.13 (m, 4H, Ar–H, *m*-to, –N=N–), 7.81–7.84(m, 4H, Ar–H, *o*-to, –N=N–), 7.89–7.92 (m, 2H, Ar–H, *o*-to, –CON–), 8.13–8.16 (d, 2H, Ar–H, *m*-to, –NO$_2$), 8.37–8.40 (d, 2H, Ar–H, *o*-to, –NO$_2$), 10.48, 10.80 (s, 2H, –CO–$\underline{\text{NH}}$–$\underline{\text{NH}}$–CO–). FTIR (KBr, pellet, cm^{-1}): 3223, $\overline{2920}$, $\overline{2851}$, 1681, 1645, 1602, 1594, 1580, 1571, 1538, 1497, 1468, 1353, 1247, 1149, 1108, 1023, 871, 842, 723, 554. Elemental analysis: calculated for $C_{43}H_{53}N_5O_7$, C 68.69, N 9.31, H 7.10; found, C 68.92, N 9.68, H 7.29%.

Using the same method, compounds **E12-10-NO$_2$**, **E1-10-NO$_2$**, **E1-6-NO$_2$** and **E1-5-NO$_2$** were successfully synthesised and characterised.

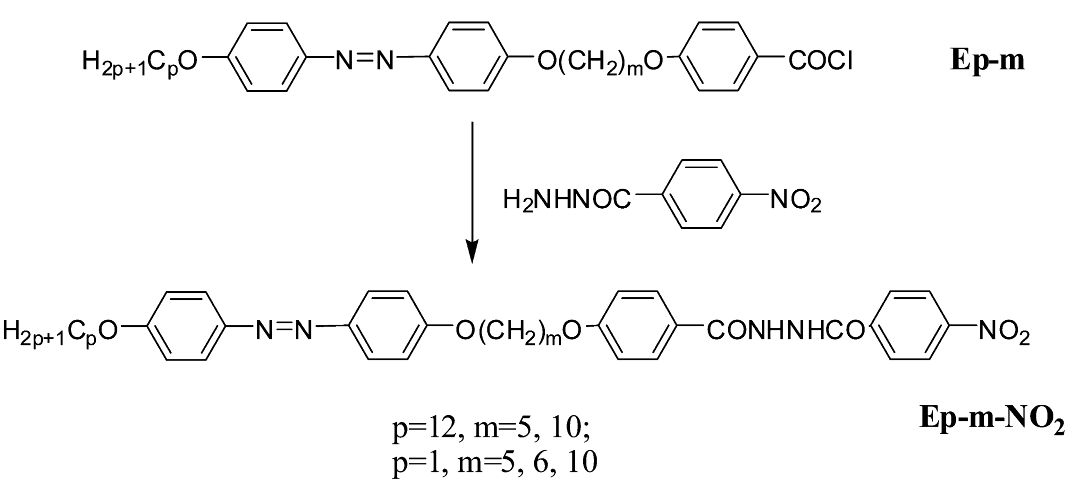

Scheme 2. The synthesis of **Ep-m-NO$_2$**.

For **E12-10-NO$_2$**, elemental analysis: calculated for $C_{48}H_{63}N_5O_7$, C 70.13, N 8.52, H 7.72; found, C 70.06, N 8.72, H 7.89%.

For **E1-10-NO$_2$**, elemental analysis: calculated for $C_{37}H_{41}N_5O_7$, C 66.55, N 10.49, H 6.19; found, C 66.85, N 10.24, H 6.47%.

For **E1-6-NO$_2$**, elemental analysis: calculated for $C_{33}H_{33}N_5O_7$, C 64.80, N 11.45, H 5.44; found, C 65.06, N 11.64, H 5.37.

For **E1-5-NO$_2$**, elemental analysis: calculated for $C_{32}H_{31}N_5O_7$, C 64.31, N 11.72, H 5.23; found, C 64.53, N 11.82, H 5.09.

Characterisation

^{1}H NMR spectra were recorded using a Mercury-300BB 300 MHz spectrometer, using DMSO-d_6 as solvent and tetramethylsilane as an internal standard. FT-IR spectra were recorded with a Perkin–Elmer spectrometer (Spectrum One B) using KBr pellets. The thermal properties of the compounds were investigated by differential scanning calorimetry (DSC) with a Mettler-Toledo DSC821^e instrument. The rate of heating and cooling was 10°C min^{-1}, the weight of the sample was about 2 mg and indium and zinc were used for calibration. The peak maximum was taken as the phase transition temperature. Optical textures were observed by polarising optical microscopy (POM) using a Leica DMLP microscope equipped with a Leitz 350 heating stage. X-ray diffraction (XRD) measurements were carried out with a Bruker Avance D8 X-ray diffractometer.

3. Results and discussion

Intermolecular hydrogen bonding in Ep-m-NO$_2$

To investigate the effect of intermolecular hydrogen bonding on the phase transitions, temperature-dependent FT-IR spectroscopy was performed on **Ep-m-NO$_2$**. Figure 1 a shows the FT-IR spectra of **E12-10-NO$_2$** at different temperatures. It can be seen that the ν(N–H) wavenumbers of **E12-10-NO$_2$** are at around 3214 and 3246 cm^{-1} in the SmA phase and isotropic phase, respectively. Apart from the main bands at 3214 (SmA phase) and 3246 cm^{-1} (isotropic phase), a shoulder peak appeared at 3395 cm^{-1} in SmA and isotropic phases, which was assigned to free ν(N–H). In addition, the C=O stretching vibrations shifted from 1690 cm^{-1} and 1656 cm^{-1} (isotropic phase) to 1671 cm^{-1} and 1594 cm^{-1} (SmA phase), respectively. The observed N–H stretching vibration frequency at 3214 cm^{-1} in the SmA phase and the increase of N–H stretching vibration by ca. 32 cm^{-1} at the isotropic transition (Figure 1(b)) strongly indicated that the presence of the hydrogen bonding in the SmA phase of **E12-10-NO$_2$** (*19, 21*).

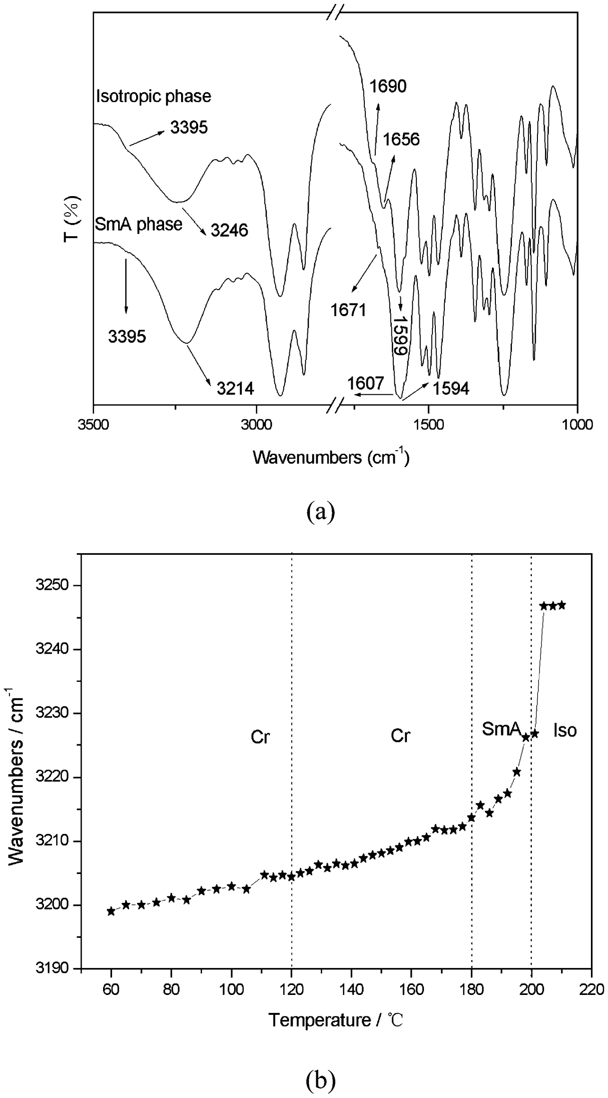

Figure 1. (a) The temperature-dependent FT-IR spectra of **E12-10-NO$_2$** on first cooling in the SmA (186°C) and isotropic (205°C) phases. (b) The temperature-dependent –NH stretching vibrations of **E12-10-NO$_2$** on first cooling (Cr, SmA and I indicate crystalline, smectic A and isotropic phases, respectively).

Phase behaviour

The phase behaviour of **Ep-m-NO$_2$** was studied by POM, DSC and powder XRD measurements. Compounds **E12-10-NO$_2$**, **E1-10-NO$_2$** and **E1-6-NO$_2$** exhibit an enantiotropic SmA phase with fan-shaped texture (Figure 2(a)) and a polygonal pattern (Figure 2(b)) is observed for **E12-5-NO$_2$**. However, no mesophase was observed for **E1-5-NO$_2$**.

The phase transition temperatures and associated enthalpies of the compounds are summarised in

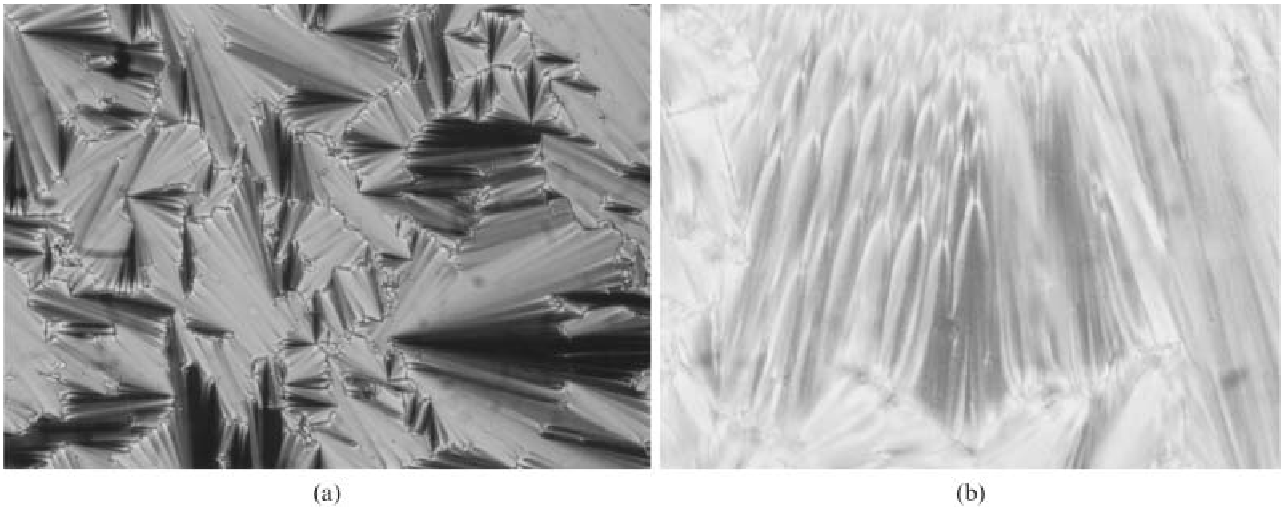
(a)

(b)

Figure 2. Polarising optical microphotographs of: (a) **E1-6-NO$_2$** at 212°C ($\times$400); (b) **E12-5-NO$_2$** at 206°C ($\times$400) on first cooling.

Table 1. Transition temperatures (°C) and enthalpies (kJ mol^{-1}, in parentheses) of **Ep-m-NO$_2$** (the rate of heating and cooling was 10°C min^{-1}).

Compound	First cooling	Second heating
E12-10-NO$_2$	I 201 (6.8) SmA 181 (29.8) Cr 120 (1.0) Cr	Cr 130 (0.8) Cr 196 (32.1) SmA 205 (6.4) I
E12-5-NO$_2$	I 217 (6.6) SmA 203 (37.0) Cr 72 (2.5) Cr	Cr 82 (3.4) Cr 215 (42.7) SmA 220 (5.4) I
E1-5-NO$_2$	I 205 (53.4) Cr	Cr 223 (54.0) I
E1-6-NO$_2$	I 226 (4.5) SmA 187 (17.8) Cr 97 (4.2) Cr	Cr 148 (3.3) Cr 211 (17.3) SmA 225 (3.2) I
E1-10-NO$_2$	--------------	Cr 145 (6.4) Cr 218 (49.7) SmA 270[a]

Cr, SmA and I indicate crystalline, smectic A and isotropic liquid phases, respectively. [a]Compound **E1-10-NO$_2$** began to decompose at about 270°C, a temperature at which the sample is still in the SmA phase according to the results of both DSC in the first heating run and POM observation.

Table 1. As can be seen from Table 1, the length of the terminal alkyl chain of the azobenzene core plays an important role in the formation of the mesophase. Compound **E12-5-NO$_2$** with **a** long alkyl chain exhibited a SmA phase, whereas **E1-5-NO$_2$** with a methyloxy substituent was non-mesomorphic. Transition temperatures of **E12-10-NO$_2$** and **E12-5-NO$_2$** with a dodecyloxy substituent are much lower than those of **E1-10-NO$_2$** and **E1-5-NO$_2$** with a methyloxy substituent, which indicates that the melting points of the compounds decrease with elongation of the terminal chains. Compared to **E1-6-NO$_2$**, which exhibits an enantiotropic SmA phase, **E1-5-NO$_2$** is non-mesomorphic.

Mesophase structure of Ep-m-NO$_2$

XRD measurements were performed on the mesophases of **Ep-m-NO$_2$**. Characteristic patterns of a smectic phase with sharp peaks in the lower-angle region and a broad halo in the higher-angle region (about 20°) were observed, as shown in Figure 3. The layer spacing values (d) collected in the Table 2 were almost independent of temperature. The layer spacings of **Ep-m-NO$_2$** were almost equal to the estimated all-trans molecular length (l) of the most extended conformation.

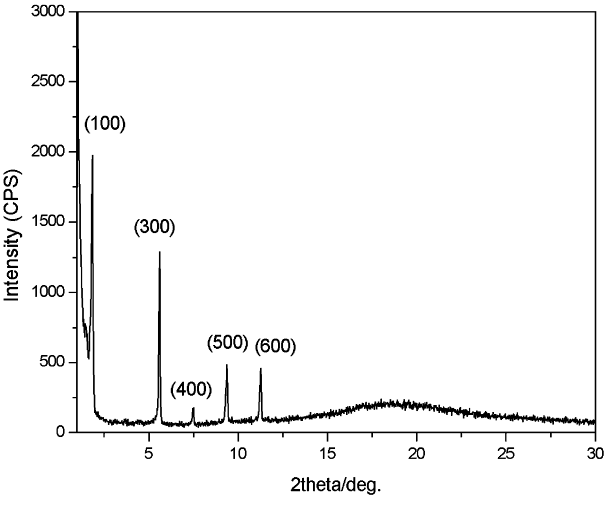

Figure 3. XRD pattern of **E12-5-NO$_2$** at 215°C.

Table 2. Summary of XRD results for **Ep-m-NO$_2$** in their mesophases.

Compounds	Molecular length l/Å	T/°C	Layer spacing d/Å	d/l
E12-10-NO$_2$	55.77	200	55.46	0.99
E12-5-NO$_2$	48.99	215	47.50	0.97
E1-6-NO$_2$	36.83	220	36.36	0.99
E1-10-NO$_2$	41.78	220	40.09	0.96

These results indicate that the molecules of **Ep-m-NO$_2$** are arranged in a monolayer with the molecular long axis along the layer normal in their liquid crystalline phases (SmA). Thus, it is reasonable to propose that the molecules in their liquid crystalline phases arrange in an alternative ways, as shown in Figure 4, in which the azobenzene part can be considered more or less as a part of one of the tails (*21, 23*). This packing model is similar to the SmA$_1$ phase of the non-symmetric rod-like hydrazide derivatives with long alkyl chain (**Cn-NO$_2$**) (*19*). Moreover, this packing model is in favour of intermolecular hydrogen bonding between the hydrazide-containing groups, which has been confirmed through variable temperature FT-IR experiments.

We have reported previously that non-symmetric liquid crystal dimers (**EmCn**, Scheme 1 a) with long terminal chains exhibit a monolayer smectic C phase, but not an intercalated smectic phase (*21*). In the present case, the non-symmetric liquid crystal dimers (**Ep-m-NO$_2$**) exhibit a SmA$_1$ phase. As has been confirmed, the onset of lateral hydrogen bonding between hydrazide groups facilitates tilting of the mesogenic groups as well as monolayer arrangement in **EmCn**. In contrast, for **Ep-m-NO$_2$**, apart from the lateral intermolecular hydrogen bonding, strong longitudinal dipole–dipole interactions between –NO$_2$ groups will further affect the intermolecular arrangement in the liquid crystalline phase, resulting in a SmA$_1$ phase.

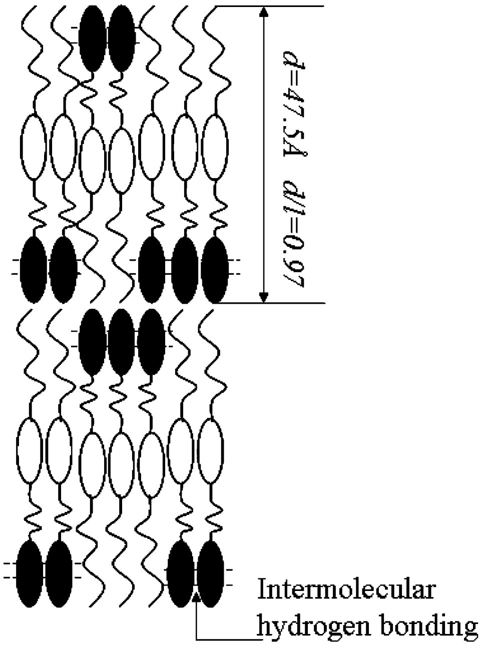

Figure 4. A sketch of the monolayer smectic A phase of **E12-5-NO$_2$** (the dashed lines indicate the lateral hydrogen bonding between mesogens; ellipse and filled ellipse represent different mesogenic groups).

In general, non-symmetric liquid crystal dimers exhibit an intercalated smectic phase (*8*), whereas symmetric liquid crystal dimers exhibit monolayer smectic phase (*1–3*). However, as shown here and previously (*21*), it is possible to observe a monolayer smectic phase with different molecular arrangement in non-symmetric liquid crystal dimers and an intercalated smectic phase in symmetric liquid crystal dimers (*20*) by introducing lateral intermolecular hydrogen bonding interactions. Based on these observations, it can be concluded that molecular arrangement in the liquid crystal dimers could be modulated through specific molecular design, such as introducing specific intermolecular interactions (e.g. hydrogen bonding and dipole–dipole interactions) and controlling the balance among different interactions.

4. Conclusion

In conclusion, a new series of non-symmetric liquid crystal dimers containing a 4-nitrobenzohydrazide group and an azobenzene group as the mesogenic units have been designed and smectic A$_1$ phases observed in these non-symmetric dimers. Lateral hydrogen bonding and strong dipole–dipole interactions are the major driving forces for the formation of the smectic A$_1$ structure. Both the lengths of terminal alkyl chains and the flexible spacers play key roles in the formation of the stable smectic phase.

Acknowledgements

The authors are grateful to the National Science Foundation Committee of China (project No. 50373016), Program for New Century Excellent Talents in Universities of China Ministry of Education, Special Foundation for PhD Program in Universities of China Ministry of Education (Project No. 20050183057) and Project 985-Automotive Engineering of Jilin University for their financial support of this work.

References

(1) Imrie C.T.; Luckhurst G.R. In *Handbook of Liquid Crystals,* Vol. 2B; Demus D., Goodby J.W., Gray G.W., Spiess H.W., Vill V. (Eds); p. 801–833; Wiley-VCH: Weinheim, 1998.

(2) Imrie C.T.; Henderson P.A. *Curr. Opin. Colloid. Interface Sci.* **2002**, *7*, 298–311.

(3) Imrie C.T. *Struct. Bonding* **1999**, *95*, 149–192.

(4) (a) Šepelj M.; Lesac A.; Baumeister U.; Diele S.; Bruce D.W.; HamerŠak Z. *Chem. Mater.* **2006**, *18*, 2050–2058; (b) Lee, W.K.; Kim, K.N.; Achard, M.F.; Jin, J.I. *J. Mater. Chem.* **2006**, *16*, 2289–2297.

(5) Blatch A.E.; Fletcher I.D.; Luckhurst G.R. *J. Mater. Chem.* **1997**, *7*, 9–17.

(6) Yelamaggad C.V.; Bonde N.L.; Achalkumar A.S.; Rao D.S.S.; Prasad S.K.; Prajapati A.K. *Chem. Mater.* **2007**, *19*, 2463–2472.

(7) Yelamaggad C.V.; Shashikala I.S.; Liao G.; Rao D.S.S.; Prasad S.K.; Li Q.; Jakli A. *Chem. Mater.* **2006**, *18*, 6100–6102.

(8) Imrie C.T. *Liq. Cryst.* **2006**, *33*, 1449–1454.

(9) (a) Hogan J.L.; Imrie C.T.; Luckhurst G.R. *Liq. Cryst.* **1988**, *3*, 645–650; (b) Lee, D.W.; Jin, J.I.; Laguerre, M.; Achard, M.F.; Hardouin, F. *Liq. Cryst.* **2000**, *27*, 145–152.

(10) (a) Attard G.S.; Date R.W.; Imrie C.T.; Luckhurst G.R.; Roskilly S.J.; Seddon J.M.; Taylor L. *Liq. Cryst.* **1994**, *16*, 529–581; (b) Wallage, M.J.; Imrie, C.T. *J. Mater. Chem.* **1997**, *7*, 1163–1167.

(11) Park Y.S.; Lee K.H.; Lee J.W.; Jin J.I. *Liq. Cryst.* **2003**, *30*, 173–179.

(12) Prasad V.; Rao D.S.S.; Prasad S.K. *Liq. Cryst.* **2001**, *28*, 761–767.

(13) Achten R.; Koudijs A.; Karczmarzyk Z.; Marcelis A.T.M.; Sudholter E.J.R. *Liq. Cryst.* **2004**, *31*, 215–227.

(14) Henderson P.A.; Seddon J.M.; Imrie C.T. *Liq. Cryst.* **2005**, *32*, 1499–1513.

(15) Demus D.; Gloza A.; Hauser H.; Rapthel I.; Wiegeleben A. *Cryst. Res. Technol.* **1981**, *16*, 1445–1451.

(16) Kutsumizu S. *Curr. Opin. Solid St. Mater. Sci.* **2002**, *6*, 537–543.

(17) Beginn U. *Prog. Polym. Sci.* **2003**, *28*, 1049–1105.

(18) Beginn U.; Lattermann G.; Festag R.; Wendorff J.H. *Acta polym.* **1996**, *47*, 214–218.

(19) Pang D.M.; Wang H.T.; Li M. *Tetrahedron* **2005**, *61*, 6108–6114.

(20) Wang H.T.; Bai B.L.; Zhang P.; Long B.H.; Tian W.J.; Li M. *Liq. Cryst.* **2006**, *33*, 445–450.

(21) Bai B.L.; Wang H.T.; Xin H.; Shi J.H.; Long B.H.; Li M. *J. Phys. Org. Chem.* **2007**, *20*, 589–593.

(22) Bai B.L.; Wang H.T.; Xin H.; Long B.H.; Li M. *Liq. Cryst.* **2007**, *34*, 659–665.

(23) Ostrovskii B.I. *Struct. Bonding* **1999**, *94*, 199–207.